View Article Online / Journal Homepage / Table of Contents for this issue

Preparation of γ-Al_2O_3 film by high temperature transformation of nanosized γ-AlOOH precursors

Yannick Mathieu, Loïc Vidal, Valentin Valtchev† and Bénédicte Lebeau*

Received (in Montpellier, France) 21st July 2009, Accepted 10th August 2009
First published as an Advance Article on the web 15th September 2009
DOI: 10.1039/b9nj00351g

Published on 15 September 2009 on http://pubs.rsc.org | doi:10.1039/B9NJ00351G
Downloaded by University of Belgrade on 02 January 2013

Mesoporous boehmite (γ-AlOOH) and gamma-alumina (γ-Al_2O_3) self-supported films were prepared by high temperature transformation of γ-AlOOH precursor fibers. A polymer, sodium polyacrylate, was used as a size/morphology controlling agent yielding to a stable colloidal suspension of boehmite ribbon-like fibers after a 168 h hydrothermal treatment at 160 °C. The slow evaporation of the solvent leads to γ-AlOOH film without any cracks and pinholes. The γ-Al_2O_3 film, obtained after calcination of the γ-AlOOH film, exhibit a high thermal stability up to 1000 °C and two distinct kinds of mesopores with average diameters of 20–30 Å and 50 Å. Structural and textural properties of these films confer them interesting properties for filtration processes.

Introduction

Inorganic porous films are of primary interest in industry due to their thermal and chemical stability, pressure resistance and longer life time in contrast to pure organic films traditionally prepared with polymers. In recent years significant attention was paid to the preparation of alumina films with tailored properties for applications in catalysis, gas separation, liquid filtration processes or medical purposes.[1–8] For instance, alumina films are known to be used as a support material in catalysis during the chemical vapour deposition of single-wall carbon nanotubes,[1] to incorporate Pd or La_2O_3–Ga_2O_3 nanoparticles for the permeation of hydrogen.[2–3] Alumina films are also recognized to have a high selectivity for the ultrafiltration of gas,[4] aqueous[5–6] or non aqueous solvents.[7] Another study reported the use of nanoporous γ-Al_2O_3 films for osteoblast culture.[8]

The aluminium oxyhydroxide known as boehmite (γ-AlOOH) is widely used as a starting material to produce γ-Al_2O_3 films. Few studies reported some applications for γ-AlOOH films mainly in coating technology for the glass surface of fluorescent lamps[9] or plastics.[10] An interesting conductivity of $1.4 \times 10^{-3}\ \Omega^{-1}\ cm^{-1}$ for a γ-AlOOH film was mentioned by Music *et al.* thus giving way to a possible application as a new solid state electrolyte.[11] Boehmite was also used to prepare super-hydrophobic films.[12–13]

As the phase transition of γ-AlOOH into γ-Al_2O_3 is topotactic, controlling morphological features of boehmite particles is of primary importance to obtain alumina films with tailored properties.

Colloidal suspensions used to prepare γ-AlOOH films were usually prepared according to the alkoxide procedure described by Yoldas.[14] However, the price of aluminium alkoxides are much higher and the toxicity of some of the byproducts (butanol) present important drawbacks for an industrial development in contrast to pure inorganic aluminium salts. Furthermore, calcination of γ-AlOOH films at high temperature (400–500 °C) often lead to the apparition of cracks or pinholes due to strong agglomeration phenomenon of the boehmite precursor particles. Therefore, numerous studies reports on the use of organic additives such as PVA or PEG to avoid cracking phenomena on alumina films.[15–17] For instance, Yang *et al.* studied several composite films obtained after slow evaporation of the solvent at room temperature for various times (9–13 days) of a PVA–boehmite solution with different compositions ranging from 7.9 to 98.2 wt% in PVA.[15] The authors observed the absence of cracks or pinholes and that the transition temperature of γ-AlOOH into γ-Al_2O_3 was delayed from 415 °C for the PVA free boehmite film to 445 °C for the 23.8 and 38.4 wt% PVA–boehmite composite films related to structural modifications of the boehmite due to the presence of the polymer. Higher PVA content (98.2 wt%) lead to the collapse of the boehmite structure. Lambert and Gonzalez[16] also studied the influence of the binder addition (PVA or PEG) on several boehmite films. The γ-AlOOH films were prepared by evaporation at room temperature of a PEG (or PVA) boehmite mixture of 2 wt% in polymer. It was found that the addition of PEG did not inhibit the presence of cracks and lead to a slight increase of the surface area of the γ-Al_2O_3 film from 360 $m^2\ g^{-1}$ (boehmite film without organic binder) to 430 $m^2\ g^{-1}$ (2 wt% in PEG) and the pore diameters from 3.6 to 5.4 nm. The contact time between the PVA polymer and the boehmite solution during the peptisation process play an important role. As longer contact times were used, *i.e.* 72 h than the traditional 24 h contact time, an increase of the adsorption of the PVA polymer on the boehmite particles was observed thus leading to a crack free γ-Al_2O_3 film after the calcination step. The γ-Al_2O_3 films exhibit a narrow pore size distribution (4–5.5 nm) and a high surface area (310–350 $m^2.g^{-1}$). Pan *et al.*

Equipe Matériaux à Porosité Contrôlée (MPC), Institut de Science des Matériaux de Mulhouse (IS2M), LRC 7228 CNRS, Université de Haute Alsace, ENSCMu-3, rue Alfred Werner, 68093 Mulhouse Cedex, France. E-mail: Benedicte.Lebeau@uha.fr
† Current address: Laboratoire Catalyse et Spectrochimie, UMR 6506 CNRS, 6 bvd du Maréchal Juin, 14050 Caen Cedex 4, France.

Published on 15 September 2009 on http://pubs.rsc.org | doi:10.1039/B9NJ00351G
Downloaded by University of Belgrade on 02 January 2013

synthesized a mesoporous spinnel $MgAl_2O_4$ exhibiting a surface area ranging from 120 to 230 $m^2\ g^{-1}$ and a pore size diameter ranging from 14.3 to 7.5 nm depending on the calcination temperature.[17] A 8 wt% PVA solution in water was also used to prevent cracks formation during the drying process and heating treatment.

Here we report a simple way to perform the synthesis of γ-AlOOH and γ-Al_2O_3 films obtained from the hydrothermal treatment of an $AlCl_3$–NaPa containing system. Recently, we have studied the factors controlling the formation of stable colloidal suspensions of boehmite nanoparticles synthesized under hydrothermal conditions.[18] Sodium polyacrylate (NaPa) was employed as a size/morphology controlling agent leading to nanoparticles with tuned properties. Thus, stable colloidal suspensions of boehmite nanoparticles ranging from 50 to 80 nm in size and from spherical to plate-like morphology were obtained. The prolongation of the synthesis time from 24 to 168 h resulted in gradual transformation of those particles in long boehmite ribbon-like fibers with a length up to 2–3 μm and a diameter of 10–15 nm. The particular morphology was used to obtain a thin transparent γ-AlOOH film free from any cracks and pinholes. The precursor γ-AlOOH film was prepared on a Petri dish using the purified boehmite colloidal suspension, which was subjected to slow evaporation of the solvent at 60 °C. Further, a thin transparent γ-Al_2O_3 film was also obtained by high temperature transformation of the γ-AlOOH film at 550 °C. The γ-AlOOH and γ-Al_2O_3 films were characterized by X-ray diffraction, nitrogen adsorption measurements, thermal analyses, transmission and scanning electron microscopy and chemical analysis.

Results and discussion

The powder sample obtained after 168 h hydrothermal treatment at 160 °C exhibited the characteristic X-ray diffraction patterns of boehmite (Fig. 1).[19] A comparison of the XRD patterns of the γ-AlOOH film with that of the powder revealed a strong enhancement of the (020) and (080) diffraction peaks, disclosing an important preferential orientation. The X-ray diffraction data of the boehmite powder, the boehmite film and a boehmite reference material (PDF N°21-1307) were summarized in Table 1. For the γ-AlOOH film, the intensity ratio of the (020) and (021) peaks ($I_{(020)}/I_{(021)} \sim 14.4$) is more than 13 times larger than the same ratio observed for the boehmite powder ($I_{(020)}/I_{(021)} \sim 1.1$). The strong enhancement of the (0k0) family peaks observed for the XRD pattern of the film indicates that the boehmite sheets are closely packed with the (0k0) plans normal to the surface. The $d_{(020)}$ values observed for the boehmite powder (0.619 nm) and film (0.609 nm) were consistent with a well crystallized boehmite material (0.611 nm, PDF N°21-1307). Numerous studies performed on the microstructure of boehmite films often revealed an apparent preferential orientation of the boehmite particles.[20–22] For instance, Ouyang *et al.* compared the XRD patterns of the powder and the film of a boehmite sample obtained from of an $AlCl_3$–NH_3 precursor mixture at ambient temperature and observed the same strong enhancement of the (020) and (080) diffraction peaks attributed to a preferential orientation of the boehmite grains.[20] Similar results were

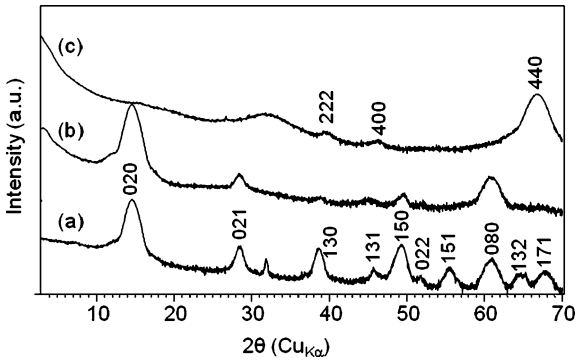

Fig. 1 XRD patterns of the boehmite powder sample synthesized for 168 h at 160 °C (a), the γ-AlOOH film (b) and γ-Al_2O_3 film (c).‡

obtained by Popa *et al.* who studied boehmite films of different thickness by XRD.[21] Furuta *et al.* also studied boehmite films obtained after evaporation of the solvent of a boehmite solution synthesized *via* hydrothermal treatment of an aqueous solution of aluminium isopropoxide (or aluminium chloride) solution.[22] A strong increase in the ratio of the (020) and (120) peaks from $I_{(020)}/I_{(120)} \sim 1.01$ for the starting boehmite material (exhibiting a fiber-like morphology) to 51.4 for the boehmite film was again observed due to the parallel orientation of boehmite fibers to the surface.

The high temperature XRD experiments performed on the boehmite powder obtained after 168 h hydrothermal treatment at 160 °C clearly showed that the phase transition from γ-AlOOH to γ-Al_2O_3 occurred for a temperature ranging from 350 to 400 °C which is in agreement with traditional values reported in the literature (Fig. 2).[23] As the calcined temperature increased from 400 to 1000 °C, γ-Al_2O_3 was the only phase detected that reflects a good thermal stability (no formation of δ-Al_2O_3 in this temperature range). It is worth mentioning that the γ-Al_2O_3 → δ-Al_2O_3 transition temperature strongly depends on the characteristic of the boehmite precursor, *i.e.* degree of crystallinity[24] or morphology and size of the particles.[25] Indeed, a crystalline boehmite often leads to γ-Al_2O_3 → δ-Al_2O_3 transition temperature around 850–950 °C whereas a highly crystalline boehmite results in a lower transition temperature around 600–700 °C.

Chemical analyses performed by X-ray fluorescence on the polymer NaPa 2100, the $AlCl_3$ + NaPa lyophilized mixture obtained at pH = 10.5 and the boehmite powder were summarized in Table 2. A strong decrease of the Na/Al and C/Al molar ratios of the boehmite powder was observed in contrast to the $AlCl_3$ + NaPa lyophilized mixture obtained at pH = 10.5. The decrease of the Na/Al and C/Al ratios from 11.86 to 0.10 and from 37.80 to 0.26, respectively, were related to the elimination of polymer NaPa after the purification performed by dialysis. The presence of C and Na in the final boehmite powder is due to small amount of NaPa in interaction with γ-AlOOH fibers. The TGA and DTA curves of the γ-AlOOH film and the sodium polyacrylate 2100 are given in Fig. 3. For the boehmite film, two distinct weight losses can be seen. The first weight loss around 10% observed between

‡ Diffractograms of γ-Al_2O_3 film were recorded with 2θ scan range of 3–80° with scan speed of 0.002° s^{-1}.

 This journal is © The Royal Society of Chemistry and the Centre National de la Recherche Scientifique 2009

Published on 15 September 2009 on http://pubs.rsc.org | doi:10.1039/B9NJ00351G
Downloaded by University of Belgrade on 02 January 2013

Table 1 X-Ray diffraction data of the boehmite powder and the boehmite film

Boehmite sample	Intensity (020) (Counts degree)	$I_{(020)}/I_{(021)}$[a]	$d_{(020)}$ (nm)	b(Å)[b]
Powder	195.7	1.1	0.619	12.37
Film	15970	14.4	0.609	12.18
Reference (PDF 21–1307)	—	1.54	0.611	12.23

[a] Intensity ratio of the (020) to (120) peaks. [b] b Unit cell parameter.

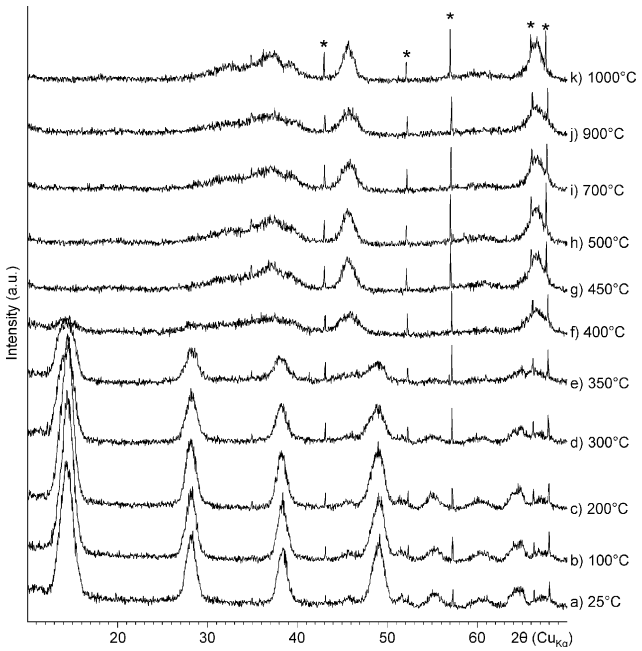

Fig. 2 High temperature XRD patterns of boehmite powder obtained after a 168 h hydrothermal treatment at 160 °C recorded with temperature-controlled chamber under conditions given in experimental section. (*: Si wafer).

about 25 and 200 °C, which is coupled with an endothermic signal associated to the elimination of physisorbed water. The second one (20.5 wt%) occurred in the range 250–450 °C with a maximum at 300 °C and is assigned to the dehydroxylation of boehmite and its transformation into γ-Al_2O_3 (2 γ-AlOOH → γ-Al_2O_3 + H_2O). This is consistent with the previous result obtained by high temperature XRD experiments indicating that the dehydroxylation takes place between 350 and 400 °C. A closer look between 450 and 500 °C reveals also another slight weight loss (~1.5 wt%) coupled with a weak exothermic peak around 470 °C related to the thermal decomposition of the residual NaPa. Indeed, as it was shown by the thermal analysis of the NaPa 2100 polymer, a major weight loss (40 wt%) was observed between 300 and 500 °C coupled with a strong exothermic peak related to the decomposition of the NaPa polymer into sodium carbonate (insert Fig. 3). However, due to an overlapping of the peaks attributed to the boehmite dehydroxylation and the thermal decomposition of residual NaPa, respectively, it is difficult to evaluate correctly this weight loss. The presence of residual NaPa polymer in the boehmite sample was also revealed by ^{13}C CP MAS NMR experiments. Indeed, the three carbon atoms of the NaPa 2100 polymer were observed in the boehmite sample showing that the polymer was anchored to the boehmite fibers (spectra not shown). Another experiment was performed by zeta potential on the NaPa-containing boehmite fibers revealing a negative surface charge ($\zeta = -42.3$ mV) at pH = 5–5.5 (= pH of the colloidal suspension), whereas, as it was mentioned in a previous paper, NaPa-free boehmite crystallites are positively charged ($\zeta = 25.7$ mV).[18] This result confirms the anchoring of NaPa on the boehmite particle surface.

The nitrogen-adsorption isotherms for the boehmite powder, the boehmite film and the γ-Al_2O_3 film are shown on Fig. 4. All of the samples exhibit a type IV isotherm with a H3 hysteresis loop for the boehmite powder and film and a H1 hysteresis loop for the γ-Al_2O_3. The specific surface area for the boehmite powder and the boehmite film are quite similar with 84 and 105 $m^2\ g^{-1}$ values, respectively. According to the BJH pore-size analysis, a large pore size distribution was observed for both the boehmite powder and film around 50 Å. An increase of the specific surface area was observed for the γ-Al_2O_3 film (S_{BET} = 186 $m^2\ g^{-1}$) which is related to the additional presence of smaller pores (average diameter around 20–30 Å) in the structure of γ-Al_2O_3 as it was shown by the BJH pore size analysis. Hg porosimetry measurements performed on the γ-AlOOH and γ-Al_2O_3 films revealed no additional porosity. The S_{BET} value of the γ-Al_2O_3 film is quite similar to other results reported in the literature for γ-Al_2O_3 films obtained *via* calcination of a boehmite film prepared after evaporation of a boehmite solution synthesized *via* hydrothermal treatment (Table 3). Using γ-AlOOH precursors obtained *via* the alcoxide procedure often lead to γ-Al_2O_3 films with higher S_{BET} values probably due to the small particle size. It is interesting to notice that the pore size diameter γ-Al_2O_3 film obtained in this work around 20–30 Å is one of the smallest reported in the literature thus giving way to interesting properties in filtration processes.

Photographs of the as-made γ-AlOOH and γ-Al_2O_3 films are shown on Fig. 5a,b. The little cracks observed on the periphery occurred during the extraction of the γ-AlOOH film from the Petri dish.

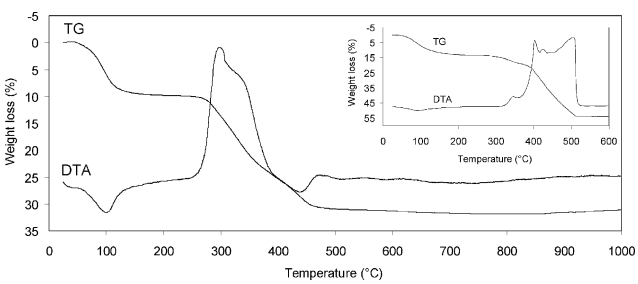

Fig. 3 TG/DTA curves of the γ-AlOOH film. Insert: TG/DTA curves of the sodium polyacrylate 2100 polymer.

Published on 15 September 2009 on http://pubs.rsc.org | doi:10.1039/B9NJ00351G
Downloaded by University of Belgrade on 02 January 2013

Table 2 Molar ratios obtained by X-ray fluorescence analysis of the NaPa 2100 polymer, the $AlCl_3$ + NaPa mixture lyophilized at pH = 10.5 and the boehmite powder

	Molar ratios		
Sample	Na/Al	Na/C	C/Al
NaPa 2100 polymer	—	0.26	—
$AlCl_3$ + NaPa lyophilized[a]	11.86	0.31	37.80
Boehmite powder[b]	0.10	0.25	0.26

[a] Obtained at pH = 10.5. [b] Obtained after washing by dialysis.

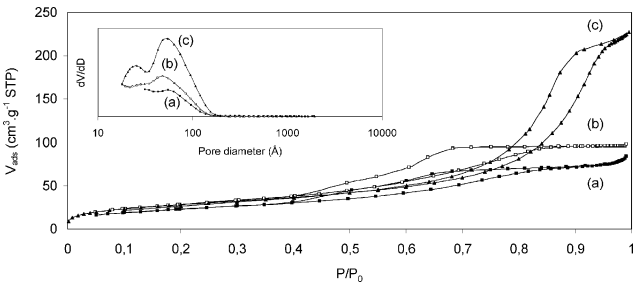

Fig. 4 Nitrogen adsorption–desorption isotherms for the boehmite powder sample synthesized for 168 h at 160 °C (a), the γ-AlOOH film (b) and the γ-Al_2O_3 film (c). Inset: The corresponding BJH pore size curves.

The TEM micrographs of the boehmite sample synthesized at 160 °C during 168 h are shown on Fig. 6. Boehmite fibers with a length ranging from 1 to 3 μm and a cross section ranging from 10 to 15 nm were obtained. A closer look at these particles reveals an unusual ribbon-like structure for a boehmite material. Films were also observed with a binocular equipped with a polarizer. A birefringent behaviour was observed for both γ-AlOOH and γ-Al_2O_3 films, which is consistent with the presence of domains with preferential orientation (Fig. 5c and d).

The γ-AlOOH film exhibits a uniform flat surface without visible cracks and pinholes (Fig. 7a). The thickness of the film was around 30 μm (Fig. 7b). A careful observation of the SEM micrographs of the fractured cross section of the γ-AlOOH film shows that the film is built up by the alignment of the long fibrous boehmite particles thus strengthening previous observations made by XRD about a preferential orientation

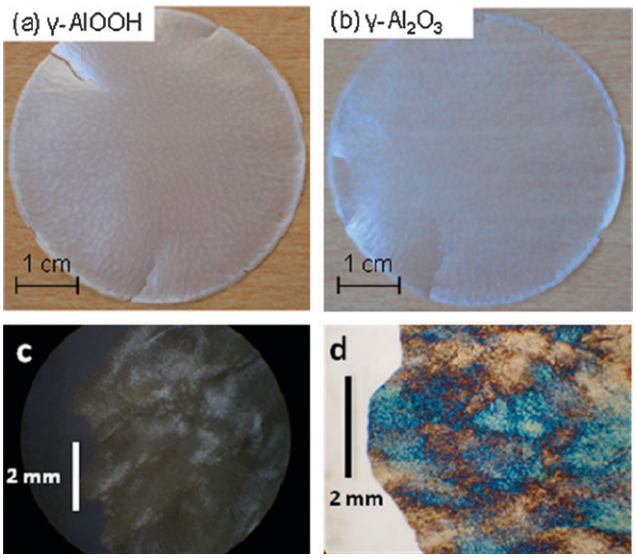

Fig. 5 Photographs of the γ-AlOOH (a) and γ-Al_2O_3 (b) films, and optical micrographs of the γ-AlOOH (c) and γ-Al_2O_3 (d) films with polarizing filter.

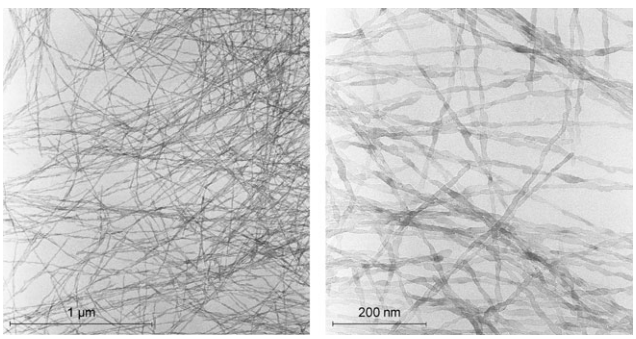

Fig. 6 TEM micrographs of the boehmite sample synthesized at 160 °C for 168 h.

phenomenon (Fig. 7c and d). As the major part of the polymer NaPa was eliminated after the purification performed by dialysis, the mechanical stability of the γ-AlOOH and γ-Al_2O_3 films (absence of cracks and pinholes) may rather be due to the specific morphology of the precursor boehmite particles than the presence of residual polymer NaPa. During

Table 3 Characteristics (synthesis procedure, surface area, pore diameter, transition temperature and nature of the polymer) of some γ-Al_2O_3 films reported in the literature

Synthesis procedure	S_{BET}/m^2 g^{-1}	Pore size diameter/nm	T_1[a]/°C	Polymer	Ref.
Alkoxide	310–350	4–5.5	445	PVA	16
Alkoxide	120–230	14.3–7.5	—	PVA	17
Alkoxide	—	4.5	—	—	26
Alkoxide	228.9	4.5	—	PVA	27
Alkoxide	137–292	8–4.4	—	PVA	28
Alkoxide	~100	8.7	—	PVA	29
Alkoxide	300–365	5.7–4.9	~300–450	PEG	30
Hydrothermal	287	—	~340	—	5
Hydrothermal	177	3.7	~400	—	4
Hydrothermal	186	2–3 and 5	~350–400	NaPa	This work

[a] Transition temperature of boehmite into γ-alumina.

 This journal is © The Royal Society of Chemistry and the Centre National de la Recherche Scientifique 2009

Published on 15 September 2009 on http://pubs.rsc.org | doi:10.1039/B9NJ00351G
Downloaded by University of Belgrade on 02 January 2013

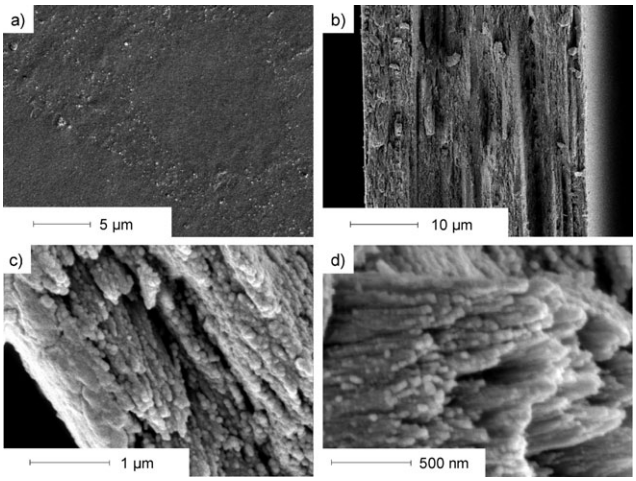

Fig. 7 SEM micrographs of the surface (a), the cross section (b) and the fractured cross sections (c,d) of the γ-AlOOH film.

the drying step of the gel, the electrostatic repulsions between boehmite fibers (negative surface charges) and the excluded volume effect lead to a preferential orientation in a nematic phase. The nematic phase in concentrated colloidal suspension of rodlike boehmite nanoparticles was observed numerous times.[31–34]

After calcination of the γ-AlOOH film at 550 °C during 6 h, the resulting γ-Al_2O_3 film also shows a uniform flat surface and the presence of cracks or pinholes was not detected which underlined the good thermal stability of this film (Fig. 8a). The thickness slightly decreased from 30 to 10 μm which is related both to the loss of water during the dehydroxylation process of the boehmite as it was shown by TG analysis and to the structural reorganization of the boehmite structure into γ-Al_2O_3 (Fig. 8b). The same alignment of γ-Al_2O_3 fibers was also observed (Fig. 8c and d). The specific morphology of the boehmite precursor particles obtained in our system and the role of the polymer NaPa which is known to inhibit the crystal growth may explain the absence of any δ-Al_2O_3 phase before 1000 °C.[18]

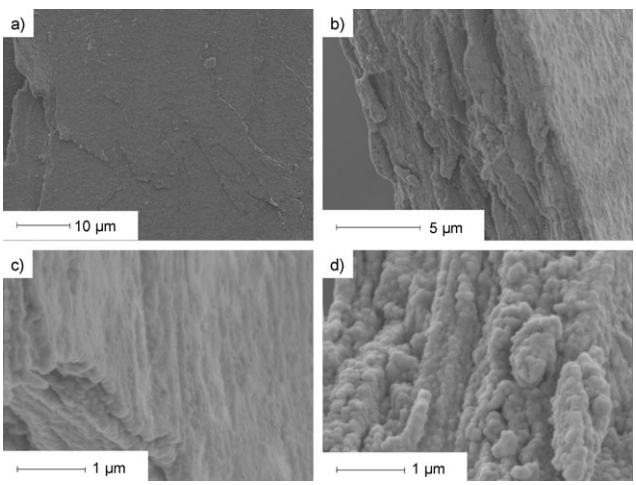

Fig. 8 SEM micrographs of the surface (a) the cross section (b,c) and the fractured cross section (d) of the γ-Al_2O_3 film.

Conclusion

This study was devoted to the preparation of self-supported mesoporous γ-Al_2O_3 films by high temperature transformation of γ-AlOOH fibers. Sodium polyacrylate was employed as a size/morphology controlling agent yielding to a stable colloidal suspension of boehmite ribbon-like fibers with a length up to 2–3 μm and a diameter of 5–8 nm after 168 h hydrothermal treatment at 160 °C which was further subjected to slow evaporation of the solvent leading to a γ-AlOOH film. The γ-Al_2O_3 film was obtained after calcination of the γ-AlOOH film at 550 °C during 6 h.

Both the γ-AlOOH and γ-Al_2O_3 showed good mechanical stability as they were free from any cracks and pinholes which is due to the ribbon-like morphology of the boehmite precursor fibers. The γ-Al_2O_3 film exhibits a high thermal stability up to 1000 °C, a specific area of 186 $m^2\ g^{-1}$ and pores size diameter of 20–30 Å and 50 Å giving way to possible applications in filtration processes.

Experimental section

Synthesis of the boehmite colloidal suspension

Sodium polyacrylate (NaPa) 2100 (Fluka) and aluminium chloride hexahydrate (Avocado) were used without further purification. The synthesis procedure includes dissolution of 9 g of NaPa 2100 in 75 ml of an aqueous solution of 0.1 M aluminium chloride. The resulting mixture was mechanically stirred at room temperature for 24 h. Sodium hydroxide (solution 5 M) was added to the $AlCl_3$ + NaPa mixture within 5 min to increase the pH up to 10.5 and the mixture was stirred for 10 more minutes. The resulting colloidal suspension was then transferred in a PTFE-lined stainless steel autoclave and heated under stirred conditions (rotating autoclave at 15 rpm) at 160 °C for 168 h. The colloidal suspension obtained after the hydrothermal treatment was then purified by dialysis with 5 L of distilled water.

Preparation of the γ-AlOOH and γ-Al_2O_3 Films

The transparent γ-AlOOH film (∅ = 8 cm, thickness = 30 μm) was obtained by slow evaporation of the solvent in a Petri dish at 60 °C for 3 days (20 ml of a γ-AlOOH colloidal suspension with an aluminium concentration of 2.8 g L^{-1}). The calcination of the γ-AlOOH film at 550 °C during 6 h yielded to a γ-Al_2O_3 transparent film.

Characterization

X-Ray powder diffraction (XRD) was performed in a reflection mode on a Philips X'Pert diffractometer (Ni filtered Cu Kα radiation anticathode, λ = 1.5408 Å) equipped with a X'Celerator detector and a temperature-controlled chamber. Diffractograms were recorded with a 2θ scan range of 3–70° at 0.02° 20 s^{-1} at 35 kV tube voltage and 55 mA tube current. A glass support was used to record the XRD of the films. High temperature X-ray diffraction experiments were performed with the same diffractometer using a Si wafer as a sample holder to record the XRD. A heating rate of 5 °C min^{-1} was

Published on 15 September 2009 on http://pubs.rsc.org | doi:10.1039/B9NJ00351G
Downloaded by University of Belgrade on 02 January 2013

used and the sample was stabilized during 30 min at the desired temperature before recording the XRD.

Chemical analyses were performed on the NaPa 2100 polymer, the $AlCl_3$ + NaPa lyophilized precursor mixture at pH = 10.5 (obtained after a 24 h freeze-drying of the precursor mixture previously frozen in N_2 liquid within 10 min) and the final boehmite powder using a X-ray fluorescence apparatus (PHILIPS MagiX). Thermal (TG/DTA) analyses were performed under air on a Setaram Labsys thermoanalyzer with a heating rate of 5 °C min^{-1} up to 1000 °C. Nitrogen adsorption measurements were carried out on a Micromeritics ASAP2010 surface area analyzer after outgassing the samples for 15 h at 150 °C. Specific surface areas and pores sizes distributions were determined by the BET and BJH methods, respectively.[35] Transmission electron microscopy (TEM) images were collected on a Philips CM200 microscope equipped with a LaB_6 filament. The accelerating voltage was 200 kV. Samples were prepared by depositing five to ten drops of the boehmite colloidal suspension onto Cu grids coated with a thin (5 nm thickness) holey carbon support film. The size and the morphology of the films were characterized by scanning electron microscopy (SEM), using a Philips XL 30 microscope. The Al concentration of the colloidal suspension was determined by Al atomic absorption spectroscopy (Varian Techtron AA6). The purification of the colloidal suspension was performed by dialysis with a Sartorius Slice 200 Benchtop instrument equipped with a 100 KD polyethersulfone film. An amount of 5 L of distilled water was used per washing. ^{13}C CP MAS NMR spectra were recorded at room temperature on a Bruker Avance II 400 spectrometer operating at B_0 = 9.4 T (Larmor frequency ν_0 = 104.26 MHz and 105.8 MHz respectively). A 4 μs pulse width was used corresponding to a flip angle of $\pi/2$ in order to ensure selective excitation of the central transition. A 2 s recycle delay was used for the analyses. Typically, 320 scans were recorded for the ^{13}C experiments. Zeta potential measurements were also performed with the Malvern ZetaSizer Nano ZS instrument using a folded capillary cell with gold electrodes (DTS1060).

Acknowledgements

Authors would like to thank Laure Michelin for X-ray fluorescence analyses and Ludovic Josien for his help in binocular observations.

References

1 H. Hongo, F. Nihey, T. Ichihashi, Y. Ochiai, M. Yudasaka and S. Iijima, *Chem. Phys. Lett.*, 2003, **380**, 158.
2 C. K. Lambert and R. D. Gonzalez, *J. Mater. Sci.*, 1999, **34**, 3109.
3 Md. H. Zahir, K. Sato, H. Mori, Y. Iwamoto, M. Nomura and S.-I. Nakao, *J. Am. Ceram. Soc.*, 2006, **89**, 2874.
4 J. Li, X. Wang, L. Wang, Y. Hao, Y. Huang, Y. Zhang, X. Sun and X. Liu, *J. Membr. Sci.*, 2006, **275**, 6.
5 K.-T. Hwang, H.-S. Lee, S.-H. Lee, K.-C. Chung, S.-S. Park and J. H. Lee, *J. Eur. Ceram. Soc.*, 2001, **21**, 375.
6 J. R. Miller and W. J. Koros, *Ind. Eng. Chem. Res.*, 1994, **33**, 934.
7 S. R. Chowdhury, D. H. A. Blank and J. E. T. Elshof, *J. Phys. Chem. B*, 2005, **109**, 22141.
8 E. E. L. Swan, K. C. Popat, C. A. Grimes and T. A. Desai, *J. Biomed. Mater. Res., Part A*, 2005, **72a**, 288.
9 V. Fraknov-Koros, *ACH–Models Chem.*, 1997, **134**, 895.
10 S. Sepeur, N. Kunze, B. Werner and H. Schmidt, *Thin Solid Films*, 1999, **351**, 216.
11 S. Music, D. Dragčević, S. Popović and A. Turković, *Mater. Lett.*, 1994, **18**, 309.
12 K. Tang, J. Yu, Y. Zhao, Y. Liu, X. Wang and R. Xu, *J. Mater. Sci.*, 2006, **16**, 1741.
13 A. Nakajima, A. Fujishima, K. Hashimoto and T. Watanabe, *Adv. Mater.*, 1999, **11**, 1365.
14 B. E. Yoldas, *Am. Ceram. Soc. Bull.*, 1975, **54**, 1856.
15 W. P. Yang, S. S. Shyu, E.-S. Lee and A.-C. Chao, *Mater. Chem. Phys.*, 1996, **45**, 108.
16 C. K. Lambert and R. D. Gonzalez, *Mater. Lett.*, 1999, **38**, 145.
17 X.-L. Pan, S.-S. Sheng, G.-X. Xiong, K.-M. Fang, S. Tudyka, N. Stroh and H. Brunner, *Colloids Surf., A*, 2001, **179**, 163.
18 Y. Mathieu, B. Lebeau and V. Valtchev, *Langmuir*, 2007, **23**, 9435.
19 R. Tettenhorst and D. A. Hofmann, *Clays Clay Miner.*, 1980, **28**, 373.
20 D. Ouyang, C. Mo and L. Zhang, *Nanostruct. Mater.*, 1996, **7**, 573.
21 A. F. Popa, S. Rossignol and C. Kappenstein, *J. Non-Cryst. Solids*, 2002, **306**, 169.
22 S. Furuta, H. Katsuki and H. Takagi, *J. Mater. Sci. Lett.*, 1994, **13**, 1077.
23 F. Schüth, K. S. Sing and J. Weitkamp, *Handbook of porous solids*, Wiley VCH, 2002, vol. 3, p. 1591.
24 P. Nortier, P. Fourre, A. B. Mohammed Saad, O. Saur and J. C. Lavalley, *Appl. Catal.*, 1990, **61**, 141.
25 I. I. M. Tijburg, H. De Bruin, P. A. Elberse and J. W. Geus, *J. Mater. Sci.*, 1991, **26**, 5945.
26 J. Buitenhuis, L. N. Donselaar, P. A. Buining, A. Stroobants and H. N. W. Lekkerkerker, *J. Colloid Interface Sci.*, 1995, **175**, 46.
27 P. A. Buining, A. P. Philipse and H. N. W. Lekkerkerker, *Langmuir*, 1994, **10**, 2106.
28 J. Buitenhuis, J. K. G. Dhont and H. N. W. Lekkerkerker, *Macromolecules*, 1994, **27**, 7267.
29 M. P. B. Van Bruggen, *Langmuir*, 2002, **18**, 7141.
30 X. Changrong, W. Feng, M. Zhaojing, L. Fanqing, P. Dingkun and M. Guangyao, *J. Membr. Sci.*, 1996, **116**, 9.
31 L. Jiansheng, W. Lianjun, H. Yanxia, L. Xiaodong and S. Xiuyun, *J. Membr. Sci.*, 2005, **256**, 1.
32 J. Schaep, C. Vandecasteele, B. Peeters, J. Luyten, C. Dotremont and D. Roels, *J. Membr. Sci.*, 1999, **163**, 229.
33 A. Nijmeijer, H. Kruidhof, R. Bredesen and H. Verweij, *J. Am. Ceram. Soc.*, 2001, **84**, 136.
34 A. L. Ahmad, C. P. Leo and S. R. A. Shukor, *J. Am. Ceram. Soc.*, 2008, **91**, 2009.
35 S. Brunauer, P. H. Emmett and E. Teller, *J. Am. Chem. Soc.*, 1938, **60**, 309.

 This journal is © The Royal Society of Chemistry and the Centre National de la Recherche Scientifique 2009